Local, Distortional, and Euler Buckling of Thin-Walled Columns

B. W. Schafer, M.ASCE[1]

Abstract: Open cross-section, thin-walled, cold-formed steel columns have at least three competing buckling modes: local, distortional, and Euler (i.e., flexural or flexural-torsional) buckling. Closed-form prediction of the buckling stress in the local mode, including interaction of the connected elements, and the distortional mode, including consideration of the elastic and geometric stiffness at the web/flange juncture, are provided and shown to agree well with numerical methods. Numerical analyses and experiments indicate postbuckling capacity in the distortional mode is lower than in the local mode. Current North American design specifications for cold-formed steel columns ignore local buckling interaction and do not provide an explicit check for distortional buckling. Existing experiments on cold-formed channel, zed, and rack columns indicate inconsistency and systematic error in current design methods and provide validation for alternative methods. A new method is proposed for design that explicitly incorporates local, distortional and Euler buckling, does not require calculations of effective width and/or effective properties, gives reliable predictions devoid of systematic error, and provides a means to introduce rational analysis for elastic buckling prediction into the design of thin-walled columns.

DOI: 10.1061/(ASCE)0733-9445(2002)128:3(289)

CE Database keywords: Thin-wall structures; Columns; Buckling; Cold-formed steel.

Introduction

Compared with conventional structural columns, the pronounced role of instabilities complicates behavior and design of thin-walled columns. Elastic buckling analysis of open cross-section, thin-walled columns typically reveal at least three buckling modes: local, distortional, and Euler. Finite strip analysis of a cold-formed steel lipped channel in pure compression (Fig. 1) shows that for practical member lengths all modes occur at stresses low enough that they must be considered in understanding and predicting behavior. Therefore, in addition to usual considerations for columns: material nonlinearity (e.g., yielding), imperfections, residual stresses, etc., the individual role and potential for interaction of buckling modes must also be considered.

Characterizing local buckling and its contribution to the degradation in strength of Euler buckling has dominated thin-walled steel column research in one form or another since the 1940's. As a result, distortional buckling was often intentionally restricted in research and ignored in design specifications. More recent work on high strength steel storage rack columns, which due to their unique geometry and elevated yield stress exhibit distortional buckling as a primary failure mode, lead to increased interest in distortional column failures (Hancock et al. 1994). A complete summary of the history of thin-walled steel column research with an emphasis on distortional buckling can be found in Schafer (2000).

Work in the last two decades has added much to our understanding of thin-walled columns, but a consistent design method that incorporates current knowledge is lacking. The combination of more refined methods for local and distortional buckling prediction, improved understanding of the postbuckling strength and imperfection sensitivity in distortional failures, and the relatively large amount of available experimental data allow for a reassessment of existing design methods and development of new procedures. Consistent integration of local, distortional and Euler buckling into the design of thin-walled columns is needed.

Elastic Local, Distortional, and Euler Buckling

Local Buckling Prediction

Closed-form prediction of local buckling is examined using two methods: the element approach and a semiempirical interaction approach. The element approach is the classic solution for buckling of an isolated plate. For lipped channel and zed columns (Fig. 2) with web depth h, flange width b, and lip length d, the critical local buckling stress ($f_{cr\ell}$) is

$$(f_{cr\ell})_{web} = k\frac{\pi^2 E}{12(1-\nu^2)}\left(\frac{t}{h}\right)^2 \quad \text{and} \quad k=4 \tag{1}$$

$$(f_{cr\ell})_{flange} = k\frac{\pi^2 E}{12(1-\nu^2)}\left(\frac{t}{b}\right)^2 \quad \text{and} \quad k=4 \tag{2}$$

$$(f_{cr\ell})_{lip} = k\frac{\pi^2 E}{12(1-\nu^2)}\left(\frac{t}{d}\right)^2 \quad \text{and} \quad k=0.43 \tag{3}$$

For the element approach, local buckling of a member, as opposed to a single element, may be approximated by taking the minimum of Eqs. (1)–(3), or weighted averages. Alternatively,

[1]Assistant Professor, 203 Latrobe Hall, Johns Hopkins Univ., Baltimore, MD 21218. E-mail: schafer@jhu.edu

Note. Associate Editor: Ronald D. Ziemian. Discussion open until August 1, 2002. Separate discussions must be submitted for individual papers. To extend the closing date by one month, a written request must be filed with the ASCE Managing Editor. The manuscript for this paper was submitted for review and possible publication on October 3, 2000; approved on July 2, 2001. This paper is part of the ***Journal of Structural Engineering***, Vol. 128, No. 3, March 1, 2002. ©ASCE, ISSN 0733-9445/2002/3-289–299/$8.00+$.50 per page.

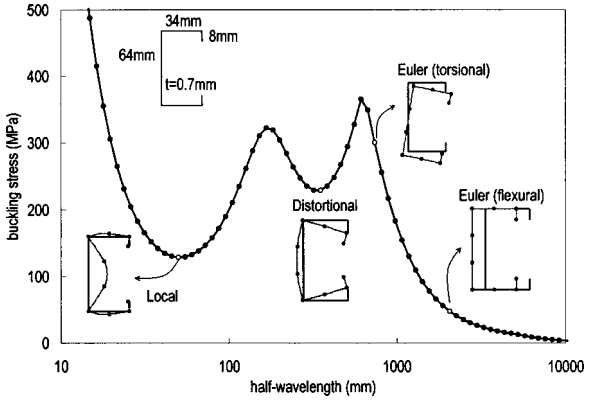

Fig. 1. Finite strip analysis of drywall stud

local interaction may be ignored and each element assumed to buckle independently; current design largely follows this approach (AISI 1996).

The semiempirical interaction approach accounts for local buckling interaction in a single connected element. Expressions for k are determined for both flange/lip local buckling and flange/web local buckling by empirical close-fit solutions to finite strip analysis results. The solutions for k [of Eq. (2)] including interactions are

$$k_{\text{flange/lip}} = -11.07\left(\frac{d}{b}\right)^2 + 3.95\left(\frac{d}{b}\right) + 4 \quad (d/b < 0.6) \tag{4}$$

$$\text{if } \frac{h}{b} \geq 1,\ k_{\text{flange/web}} = 4\left(\frac{b}{h}\right)^2\left[2 - \left(\frac{b}{h}\right)^{0.4}\right] \tag{5}$$

$$\text{if } \frac{h}{b} < 1,\ k_{\text{flange/web}} = 4\left[2 - \left(\frac{h}{b}\right)^{0.2}\right] \tag{6}$$

Local buckling of the entire member ($f_{cr\ell}$) may be predicted by taking the minimum of Eq. (4) and the appropriate expression from Eq. (5) or (6) and substituting into Eq. (2).

Distortional Buckling Prediction

Methods for closed-form prediction in the distortional mode include Desmond et al. (1981) as employed in North American design specifications (AISI 1996), and Lau and Hancock (1987) as employed in Australian/New Zealand design practice. Closed-form prediction of distortional buckling of beams is derived in Schafer and Peköz (1999); extension of this method to columns is completed here.

The rotational stiffness (k_ϕ) at the juncture of the flange and the web may be expressed as the summation of the elastic and stress dependent geometric stiffness terms with contributions from both the flange and the web:

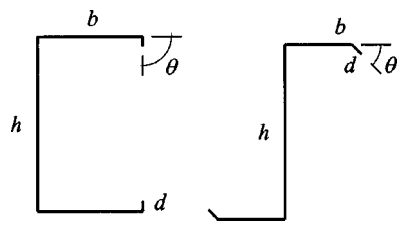

Fig. 2. Geometry of members

$$k_\phi = (k_{\phi f} + k_{\phi w})_e - (k_{\phi f} + k_{\phi w})_g \tag{7}$$

Buckling ensues when the elastic stiffness at the web/flange juncture is eroded by the geometric stiffness, i.e., when

$$k_\phi = 0 \tag{8}$$

If the stress dependent portion of the geometric stiffness is linearized and written explicitly then the critical buckling stress for distortional buckling (f_{crd}) may be found as

$$k_\phi = k_{\phi fe} + k_{\phi we} - f(\tilde{k}_{\phi fg} + \tilde{k}_{\phi wg}) = 0 \tag{9}$$

$$f_{\text{crd}} = \frac{k_{\phi fe} + k_{\phi we}}{\tilde{k}_{\phi fg} + \tilde{k}_{\phi wg}} \tag{10}$$

Expressions for the flange remain unchanged from that of the previously derived work on beams, therefore,

$$k_{\phi fe} = \left(\frac{\pi}{L}\right)^4\left[EI_{xf}(x_o - h_x)^2 + EC_{wf} - E\frac{I_{xyf}^2}{I_{yf}}(x_o - h_x)^2\right] + \left(\frac{\pi}{L}\right)^2 GJ_f \tag{11}$$

$$\tilde{k}_{\phi fg} = \left(\frac{\pi}{L}\right)^2\left\{A_f\left[(x_o - h_x)^2\left(\frac{I_{xyf}}{I_{yf}}\right)^2 - 2y_o(x_o - h_x) \times \left(\frac{I_{xyf}}{I_{yf}}\right) + h_x^2 + y_o^2\right] + I_{xf} + I_{yf}\right\} \tag{12}$$

All expressions with the subscript f (I_{xf}, I_{yf}, J_f, etc.) refer to section properties for the flange alone. Explicit expressions for all quantities in Eqs. (11) and (12) are provided in Schafer and Peköz (1999).

For columns, the web contributes rotational stiffness at both ends (i.e., both flanges buckle in the distortional mode as shown in Fig. 1) as opposed to the web of beams where rotation is only considered at one end (i.e., only the compression flange buckles). The rotational stiffness contribution of the web at the web/flange juncture is assumed equal at each end. The mechanical model employed for the web is a single, simply supported, lower order, plate bending, finite strip [see Cheung and Tam (1998) for finite strip derivations]. For the case where the lateral translation of the web at the web/flange juncture is restrained, expressions simplify greatly:

$$k_{\phi we} = \frac{Et^3}{6h(1-\nu^2)} \tag{13}$$

$$\tilde{k}_{\phi wg} = \left(\frac{\pi}{L}\right)^2\frac{th^3}{60} \tag{14}$$

Considering the lateral translation of the web at the web/flange juncture free leads to overly conservative predictions of the distortional buckling stress and is thus not detailed here.

Determination of the critical length for distortional buckling of columns follows that of the previous derivation for beams, with appropriate substitutions reflecting Eqs. (13) and (14). The resulting critical length is

$$L_{\text{cr}} = \left\{\frac{6\pi^4 h(1-\nu^2)}{t^3}\left[I_{xf}(x_o - h_x)^2 + C_{wf} - \frac{I_{xyf}^2}{I_{yf}}(x_o - h_x)^2\right]\right\}^{1/4} \tag{15}$$

The elastic distortional buckling stress (f_{crd}) is found by determining the critical length L_{cr} using Eq. (15), substituting $L = L_{\text{cr}}$

Table 1. Summary of Member Geometry

	h/b		h/t		b/t		d/t		
	max	min	max	min	max	min	max	min	Count
Selected columns for elastic buckling study									
C and *Z*—Schafer (1997) members	3.0	1.0	90	30	90	30	15.0	2.5	32
C—Commercial drywall studs	4.6	1.2	318	48	70	39	16.9	9.5	15
C—AISI Manual *C*'s	7.8	0.9	232	20	66	15	13.8	3.2	73
Z—AISI Manual *Z*'s	4.2	1.7	199	32	55	18	20.3	5.1	50
Selected columns for experimental study									
C—Loughlan (1979)	5.0	1.6	322	91	80	30	33	11	33
C—Miller and Peköz (1994)	4.6	2.5	170	46	38	18	8	5	19
C—Mulligan (1983)	2.9	1.0	207	93	93	64	16	14	13
C—Mulligan (1983) stub columns	3.9	0.7	353	65	100	33	22	7	24
C—Thomasson (1978)	3.0	3.0	472	207	159	69	32	14	13
Z—Polyzois and Charnvarnichborikarn (1993)	2.7	1.5	137	76	56	30	36	0	85

into Eqs. (11)–(14) to determine the appropriate rotational stiffness terms and then using Eq. (10) to calculate the buckling stress.

Euler Buckling Prediction

Closed-form predictions of the Euler buckling modes for *x* axis and *y* axis flexural buckling as well as flexural-torsional buckling are given in current design specifications (e.g., AISI 1996). The details of the prediction methods for doubly, singly, and point-symmetric sections are presented in Yu (2000).

Accuracy of Elastic Buckling Models

Accuracy of the closed-form methods for prediction of local and distortional buckling is assessed via finite strip analysis. The geometry of the studied members is shown in Fig. 2, and summarized in Table 1. Results are given in Table 2. For local buckling prediction the semiempirical interaction model [Eqs. (4)–(6)] is more accurate than the element model [Eqs. (1)–(3)]. For distor-tional buckling prediction current design specifications (AISI 1996) are flawed or inapplicable and both Lau and Hancock (1987) and the proposed method [Eqs. (7)–(15)] work reasonably well.

Local buckling prediction by the element model is only appropriate when the web depth (h) and flange width (b) are approximately equal ($h \cong b$). For lip lengths (d) in current practice, the error in the element model is essentially independent of d and only a function of h/b. The accuracy of the semiempirical interaction model is greatest for h/b ratios between 2 and 6.

Distortional buckling prediction by the proposed method [Eqs. (7)–(15)] has less variation, but is less conservative than Lau and Hancock (1987). For members with slender webs and small flanges the Lau and Hancock (1987) approach conservatively converges to a buckling stress of zero (note, members with zero buckling stress are not included in the summary statistics of Table 2). However, for the same members, the proposed method converges to the expected solution: equal to or slightly above the web local buckling stress. The proposed method provides a more accurate treatment of the web's contribution to the rotational stiffness at the web/flange juncture.

Table 2. Performance of Prediction Methods for Elastic Buckling

	Local				Distortional					
Average (stand. dev.)	$\frac{(f_{cr})_{true}}{(f_{cr})_{element}}$		$\frac{(f_{cr})_{true}}{(f_{cr})_{interact}}$		$\frac{(f_{cr})_{true}}{(f_{cr})_{Schafer}}$		$\frac{(f_{cr})_{true}}{(f_{cr})_{Hancock}}$		$\frac{(f_{cr})_{true}}{(f_{cr})_{AISI}}$	
All data	**1.34**	(0.13)	**1.03**	(0.06)	**0.93**	(0.05)	**0.96**	(0.06)	**0.79**	(0.33)
Schafer (1997) members	**1.16**	(0.15)	**1.02**	(0.08)	**0.92**	(0.07)	**0.96**	(0.06)	**1.09**	(0.16)
Commercial drywall studs	**1.38**	(0.09)	**1.07**	(0.05)	**0.93**	(0.02)	**1.00**	(0.07)	**0.81**	(0.26)
AISI Manual *C*'s	**1.33**	(0.13)	**1.01**	(0.07)	**0.93**	(0.05)	**0.99**	(0.03)	**0.81**	(0.26)
AISI Manual *Z*'s	**1.39**	(0.03)	**1.04**	(0.04)	**0.92**	(0.03)	**0.92**	(0.06)	**0.41**	(0.18)

Note: $(f_{cr})_{true}$ = local or distortional buckling stress from finite strip analysis.

$(f_{cr})_{element}$ = minimum local buckling stress of the web, flange, and lip via Eqs. (1)–(3).

$(f_{cr})_{interact}$ = minimum local buckling stress using the semiempirical equations [Eqs. (4)–(6)].

$(f_{cr})_{Schafer}$ = distortional buckling stress via Eqs. (7)–(15).

$(f_{cr})_{Hancock}$ = distortional buckling stress via Lau and Hancock (1987).

$(f_{cr})_{AISI}$ = buckling stress for edge stiffened element via AISI (1996) from Desmond (1981).

Ultimate Strength

Numerical Studies on Distortional Failures

Nonlinear finite element analysis of an isolated flange and lip, compressed to failure, is reported in Schafer and Peköz (1999). The ABAQUS model uses nine-node reduced integration shell elements, elastic-plastic material with strain hardening, and imperfections and residual stresses as suggested in the modeling guidelines for cold-formed steel by Schafer and Peköz (1998a). Failure mechanisms can be associated with either the local or distortional mode through examination of the locations of plastic strain at failure. From this analysis it is concluded that: distortional failures have lower postbuckling capacity than local failures, distortional buckling may control the failure mechanism even when the elastic distortional buckling stress (f_{crd}) is higher than the elastic local buckling stress ($f_{\text{cr}\ell}$), and distortional failures have higher imperfection sensitivity.

Further finite element analyses on lipped channel columns are conducted to examine the applicability of these conclusions to full members. The geometry of the selected members is summarized as the Schafer (1997) members in Table 1. The length of the members is selected as two to three times the half-wavelength of the distortional mode. Other modeling assumptions are similar to those cited for the previous analysis. The above conclusions are supported; except that reduction of the postbuckling capacity for distortional failures is less in the members than observed in models of the isolated flange and lip.

Implications of these findings for design include: the distortional mode requires a more conservative column (strength) curve than the local mode, lower ϕ factors may be needed to account for heightened imperfection sensitivity, and since elastic buckling is not a direct indicator of the final failure mode—complications may arise in correct prediction of the actual failure mode.

Experimental Studies on Distortional Failures of Rack Columns

The most extensive experimental work on the strength of cold-formed steel columns failing in the distortional mode is from the University of Sydney: Lau and Hancock (1987), Kwon and Hancock (1992), Hancock et al. (1996). Compression tests were conducted on (a) lipped channels, (b) rack column uprights, (c) rack column uprights with additional outward edge stiffeners, (d) hats, and (e) lipped channels with a web stiffener as shown in Fig. 3. The column curve fit to the distortional buckling failures may be expressed as

$$\frac{P_{nd}}{P}=\left(1-0.25\left(\frac{P_{\text{crd}}}{P}\right)^{0.6}\right)\left(\frac{P_{\text{crd}}}{P}\right)^{0.6} \quad \text{where}$$

$$\sqrt{\frac{P}{P_{\text{crd}}}} \quad >0.561, \text{ otherwise } P_{nd}=P \qquad (16)$$

where P_{nd}=nominal capacity in distortional buckling; P=squash load ($P=P_y=A_g f_y$) when interaction with other modes is not considered, otherwise $P=A_g f$, where f is the limiting stress of a mode that may interact with distortional buckling; P_{crd}=critical elastic distortional buckling load ($A_g f_{\text{crd}}$). Fig. 3 provides strong evidence that if failure is known to occur in the distortional mode, then the elastic distortional buckling load (stress) may be used to directly predict the ultimate strength.

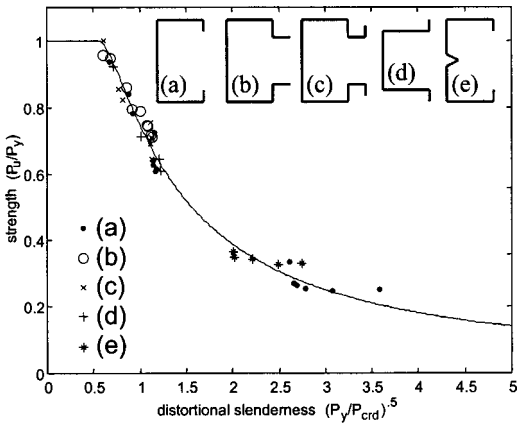

Fig. 3. Ultimate strength of columns failing in distortional buckling (Univ. of Sydney tests)

Experiments on Lipped Channel and Zed Columns

To evaluate existing and proposed methods for the design of cold-formed steel columns experimental data on lipped channel and zed columns are gathered (Thomasson 1978; Loughlan 1979; Mulligan 1983; Peköz 1987; Polyzois and Charnvarnichborikarn 1993; Miller and Peköz 1994). Only unperforated lipped channel and zed sections, with 90° edge stiffeners, tested in a pin-pin configuration are selected. The geometry of the tested sections is summarized in Table 1. The tests on lipped channels by Miller and Peköz (1994) and lipped zeds by Polyzois and Charnvarnichborikarn (1993) are not part of the experimental database used to calibrate the existing cold-formed steel specification (AISI 1996) and therefore provide an independent check.

The available experimental data on lipped channels represent a wide variety of sections: slender webs, slender flanges, and relatively long lips are all included. However, in 95 out of 102 members, h/b is greater than 1.6. Therefore, in most members the local buckling stress is lower than the distortional buckling stress due to the high slenderness of the web (only members with small lip length are an exception). For the lipped zed columns h/b ratios are similar to those of the lipped channels—thus this data suffers from the same limitations. However, the researchers specifically investigated the case of small, or no edge stiffening lip. For short lip length (small d) distortional buckling may control failure, even when the h/b ratio is high. For typical rack columns or other sections approaching a more square configuration ($h/b \cong 1$) available data is incomplete, but University of Sydney tests on high strength steel members provides an indication of strength (see Fig. 3).

Experiments on Lipped Channels with Web Stiffeners

Thomasson (1978) tested a series of cold-formed columns with up to two stiffeners in the web, with geometry as shown in Fig. 4 and summarized in Table 3. (The members without intermediate web stiffeners are included in the group of experimental data on lipped channels of the previous section.) Thomasson investigated channels with slender webs, flanges, and lips—thickness was as low as 0.63 mm (0.025 in.). Fig. 4 shows the attachments Thomasson made to the lips of the channels with intermediate web stiffeners. When Thomasson initially tested the specimens with an intermediate stiffener they buckled in a distortional mode:

> ''The provision of one or two stiffeners in the wide flange [the web] confers on the panel both an elevated load bear-

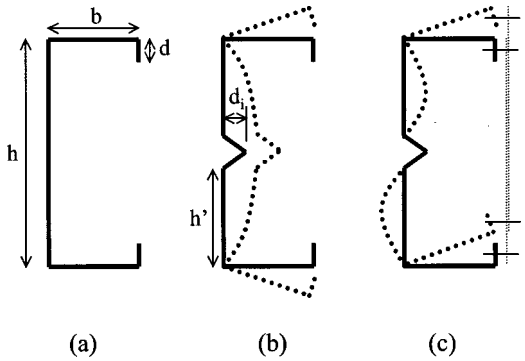

Fig. 4. Geometry of lipped channels tested by Thomasson (1978), with distortional buckling mode observed in initial testing with web stiffener in place (b) and mode observed after addition of flat bars connecting lip stiffeners (c)

ing capacity and an elevated stiffness. The consequences of improving the stiffness of the wide flange were not entirely favorable . . . . In order that the improved properties of the wide flange may be utilized, steps must be taken to prevent the occurrence of the torsional mode. By connecting the narrow flanges of the panels by means of 30×3 mm flats at 300 mm centers, the symmetrical torsion mode [Fig. 4(b)] was eliminated. This measure does not prevent the occurrence of the antisymmetrical mode [Fig. 4(c)].'' Thomasson (1978)

Partial or complete restriction of the distortional buckling mode in experiments is common in much of the earlier column research. This unique experimental data is used to help gauge the adequacy of extending proposed design procedures to members with intermediate stiffeners, and those where bracing eliminates one mode, Fig. 4(b), but allows another, Fig. 4(c).

Column Design Methods

Current thin-walled column design requires identification of the failure mode/mechanism of interest (e.g., local buckling), determination of elastic buckling characteristics for that mode (e.g., $f_{cr\ell}$), and finally calculation of ultimate strength using empirical expressions that are a function of material behavior (e.g., f_y) and the elastic buckling behavior (e.g., $f_{cr\ell}$). The failure mode(s)/mechanism(s) of potential interest for a thin-walled lipped channel or zed column include: local, distortional, and Euler buckling, as well as local interaction with distortional, local interaction with Euler, and distortional interaction with Euler, and all three modes: local, distortional, and Euler interacting.

For a given mode, the elastic buckling calculations may be organized into two groups: (1) element methods, e.g., Eqs. (1)–(3) for local buckling or (2) member methods, which include closed-form expressions [e.g., Eqs. (4)–(6) for local buckling, Eqs. (7)–(15) for distortional buckling] and numerical methods (e.g., finite strip analysis or finite element analysis).

Ultimate strength calculation generally includes one of two basic approaches: effective width or column curve/''direct strength'' methods. Effective width uses empirical expressions to determine the portion of an element which is effective in resisting the load at the full applied stress (an element is a part of a member: i.e., the flange, web, lip, etc.). For example, the effective width method, for an element of width b, commonly implemented in design specifications is

$$\frac{b_{\text{eff}}}{b}=\left(1-0.22\sqrt{\frac{f_{cr\ell}}{f}}\right)\left(\sqrt{\frac{f_{cr\ell}}{f}}\right) \quad \text{where}$$

$$\sqrt{\frac{f}{f_{cr\ell}}} \quad >0.673, \quad \text{otherwise} \quad b_{\text{eff}}=b \tag{17}$$

where b_{eff}=effective width of an element with gross width b; f=yield stress ($f=f_y$) when interaction with other modes is not considered, otherwise f is the limiting stress of a mode interacting with local buckling; $f_{cr\ell}$=critical elastic local buckling stress.

Column curve, or ''direct strength'' methods use gross properties of a member to determine the reduced strength of a column in a given mode due to buckling and/or yielding. Column curves have been typically applied to Euler buckling modes such as

$$P_{ne}=A_g f_n \quad \text{for } \lambda_c \leqslant 1.5, \quad f_n=(0.658^{\lambda_c^2})f_y$$

$$\text{for } \lambda_c>1.5, \quad f_n=\left(\frac{0.877}{\lambda_c^2}\right)f_y \tag{18}$$

where P_{ne}=nominal capacity in Euler (flexural, or flexural-torsional) buckling; $\lambda_c=\sqrt{f_y/f_e}$, and f_e=Euler buckling stress (minimum of flexural and flexural-torsional modes, with appropriate braced lengths, etc.); f_y=yield stress. Direct strength methods are the extension of column curves to other modes such as local and distortional buckling, e.g., Eq. (16) is a direct strength solution for distortional buckling. Based on existing work for beams (Schafer and Peköz 1998b), the following form is suggested for local buckling of columns:

$$\frac{P_{n\ell}}{P}=\left[1-0.15\left(\frac{P_{cr\ell}}{P}\right)^{0.4}\right]\left(\frac{P_{cr\ell}}{P}\right)^{0.4} \quad \text{where}$$

$$\sqrt{\frac{P}{P_{cr\ell}}}>0.776, \quad \text{otherwise} \quad P_{n\ell}=P \tag{19}$$

Table 3. Summary of Geometry of Lipped Channels Tested by Thomasson (1978)

	h/b		h/t		b/t		d/t		
	max	min	max	min	max	min	max	min	count
Thomasson (1978)	3.1	3.0	489	205	160	68	33	14	46
					d_i/d		h'/t		
					max	min	max	min	count
	no intermediate web stiffeners				—	—	—	—	14
	one intermediate web stiffener				0.94	0.39	222	91	16
	two intermediate web stiffeners				0.94	0.47	145	57	16

where $P_{n\ell}$=nominal capacity in local buckling; P=squash load ($P=P_y=A_g f_y$) when interaction with other modes is not considered, otherwise $P=A_g f$, where f=limiting stress of a mode that may interact with distortional buckling; $P_{cr\ell}$=critical elastic local buckling load ($A_g f_{cr\ell}$).

Effective width and direct strength design methods are assessed using the experimental data. Three different assumptions on the level of interaction between local (L), distortional (D), and Euler (E) modes are considered. Methods "B#" consider L+E interaction but D is assumed not to interact with other modes. Methods "C#" assume L+E and D+E interaction. Methods "D#" assume L+D interaction and L+E, and D+E interaction. Simultaneous L+D+E interaction is not considered in any of the methods. For example, interaction with Euler buckling is completed by limiting f used in Eqs. (16), (17), or (19) to f_n of Eq. (18). With this approach individual modes are not, and need not be, considered separately if interaction in that mode is already considered. Details of the eleven considered methods are:

A1: Current practice (AISI 1996)
- **L+E:** $P_{n\ell}=A_e f_n$, $A_e=t\Sigma b_{\text{eff}}$, b_{eff} per Eq. (17), $f_{cr\ell}$ per AISI (1996), $f=f_n$ via Eq. (18)

A2: Current practice with a distortional check
- **L+E:** $P_{n\ell}$ same as A1
- **D:** P_{nd} via Eq. (16)* with f_{crd} per Eqs. (7)–(15) and $f=f_y$

B1: Effective width with L+E and D interactions considered
- **L+E:** $P_{n\ell}=A_e f_n$, $A_e=t\Sigma b_{\text{eff}}$, b_{eff} per Eq. (17), $f_{cr\ell}$ per Eqs. (1)–(3), $f=f_n$ via Eq. (18)
- **D:** P_{nd} same as A2

B2: Direct strength (hand) with L+E and D interactions
- **L+E:** $P_{n\ell}$ per Eq. (19) with $f_{cr\ell}$ per Eqs. (4)–(6) and $f=f_n$ via Eq. (18)
- **D:** P_{nd} via Eq. (16) with f_{crd} per Eqs. (7)–(15) and $f=f_y$

B3: Direct strength (numeric) with L+E and D interactions
- **L+E:** $P_{n\ell}$ per Eq. (19) with $f_{cr\ell}$ per finite strip and $f=f_n$ via Eq. (18)
- **D:** P_{nd} via Eq. (16) with f_{crd} per finite strip and $f=f_y$

C1: Effective width with L+E and D+E interactions
- **L+E:** $P_{n\ell}$ same as B1
- **D+E:** P_{nd} via Eq. (16)* with f_{crd} per Eqs. (7)–(15) and $f=f_n$ via Eq. (18)

C2: Direct strength (hand) with L+E and D+E interactions
- **L+E:** $P_{n\ell}$ same as B2
- **D+E:** P_{nd} via Eq. (16) with f_{crd} per Eqs. (7)–(15) and $f=f_n$ via Eq. (18)

C3: Direct strength (numeric) with L+E and D+E interactions
- **L+E:** $P_{n\ell}$ same as B3
- **D+E:** P_{nd} via Eq. (16) with f_{crd} per finite strip and $f=f_n$ via Eq. (18)

D1: Effective width with L+D, L+E, and D+E interactions
- **L+D:** $P_{n\ell}=A_e f_n$, $A_e=t\Sigma b_{\text{eff}}$, b_{eff} per Eq. (17), $f_{cr\ell}$ per Eqs. (1)–(3), $f=P_{nd}/A_g$ via Eq. (16)*
- **L+E:** $P_{n\ell}$ same as C1
- **D+E:** P_{nd} same as C1

D2: Direct strength (hand) with L+D, L+E, and D+E
- **L+D:** $P_{n\ell}$ per Eq. (19) with $f_{cr\ell}$ per Eqs. (4)–(6) and $f=P_{nd}/A_g$ via Eq. (16), f_{crd} per Eqs. (7)–(15)
- **L+E:** $P_{n\ell}$ same as C2
- **D+E:** P_{nd} same as C2

D3: Direct strength (numeric) with L+D, L+E, and D+E
- **L+D:** $P_{n\ell}$ per Eq. (19), $f_{cr\ell}$ per finite strip and $f=P_{nd}/A_g$ via Eq. (16), f_{crd} per finite strip
- **L+E:** $P_{n\ell}$ same as C3
- **D+E:** P_{nd} same as C3

* This method uses a close-fit approximation to Eq. (16), by reducing f_{crd} in a manner such that b_{eff} using Eq. (17) is the same as that if Eq. (16) had been used directly—this is done such that the same effective width expression used in AISI (1996) can be used for local and distortional modes. Schafer (2000) provides complete design examples for all of the considered methods.

Performance of Design Methods

The performance of the design methods is primarily assessed by comparison to the gathered experimental data on lipped channels and zed columns and is summarized in Table 4. The University of Sydney experiments (Fig. 3) and the Thomasson (1978) experiments with intermediate web stiffeners are only considered in reference to methods B3 and C3.

Current Practice (A1)

Current design specifications (AISI 1996) employ an element based effective width approach to accommodate local buckling. Interaction with Euler buckling is handled by limiting the maximum stress in the effective width determination [f in Eq. (17)] to the nominal Euler buckling stress [f_n in Eq. (18)] Local web/flange interaction is ignored, distortional buckling is not explicitly considered, nor is interaction between distortional buckling and other modes considered.

For common lipped channels and zeds average performance is 6% unconservative. Lack of an explicit treatment for distortional buckling does not introduce significant error for common members. However, ignoring local web/flange interaction results in systematic error. Members with high web slenderness (h/t) consistently give unconservative predictions. Members with high h/t and h/b also suffer from systematically unconservative predictions. For local buckling in element approaches, as used in current design (as well as methods B1, C1, and D1) no matter how slender the web becomes it has no effect on the solution for the flange.

The experimental data on zed sections further highlights these issues, and also demonstrates additional difficulties with empirical expressions in current use. Considering Fig. 5, for small lip length (d), when distortional buckling controls, predictions are adequate. However, for intermediate d, as behavior transitions from distortional to local buckling, predictions may be significantly unconservative (e.g., $d\sim 20$ in Fig. 5) due to ignoring local web/flange interaction. Finally, for large d, predicted strength is overly conservative—and generally follows the opposite trend of the tests. The empirical correction from Desmond et al. (1981) used in current design to account for local flange/lip interaction is not supported by this data. While "on average" current methods may be adequate, systematic errors exist and can be rectified.

Current Practice with Addition of Distortional Check (A2)

For common members the addition of a separate distortional buckling check to current methods does not significantly benefit prediction. Errors for common lipped channel and zed members relate primarily to local web/flange interaction. However, rack sections, sections with intermediate web stiffeners, high strength steel members, and other shapes more prone to distortional buckling do require accurate design methods. These members would

Table 4. Test to Predicted Ratios for all Solution Methods by Controlling Limit State

Design method:	A1: AISI (1996) Specification			A2: AISI (1996) Spec. with Dist. Check					
Limit State[a]	L+E			L+E			D		
Test to predicted[b]	**mean**	std	*n*	**mean**	std	*n*	**mean**	std	*n*
Loughlan (1979)	**0.97**	0.04	13	**0.97**	0.04	13			
Miller and Peköz (1994)	**0.86**	0.04	13	**0.86**	0.04	13			
Mulligan (1983)	**0.86**	0.12	33	**0.86**	0.12	33			
Mulligan Stub col.	**1.05**	0.06	24	**1.06**	0.06	20	**1.10**	0.09	4
Thomasson (1978)	**0.99**	0.23	19	**1.00**	0.24	18	**0.98**		1
Polyzois and Charnvarnichborikarn (1993)	**0.93**	0.10	85	**0.92**	0.10	60	**1.12**	0.12	25
All data	**0.94**	0.13	187	**0.93**	0.13	1.57	**1.11**	0.11	30

Design method:	B1: Effective Width with L+E and D Check						B2: Hand-Direct Strength with L+E & D						B3: Numerical Direct Strength with L+E & D					
Limit state[a]	L+E			D			L+E			D			L+E			D		
Test to predicted[b]	**mean**	std	*n*	**mean**	std	*n*	**mean**	std	*n*	**mean**	std	*n*	**mean**	std	*n*	**mean**	std	*n*
Loughlan (1979)	**0.97**	0.04	13				**1.11**	0.07	13				**1.08**	0.07	13			
Miller and Peköz (1994)	**0.86**	0.04	13				**1.01**	0.07	13				**0.99**	0.06	12	**1.09**		1
Mulligan (1983)	**0.83**	0.12	33				**0.94**	0.12	33				**0.92**	0.13	33			
Mulligan stub col.	**1.05**	0.06	19	**1.10**	0.07	5	**1.15**	0.09	24				**1.10**	0.09	20	**1.28**	0.04	4
Thomasson (1978)	**1.00**	0.24	18	**0.98**		1	**1.01**	0.22	19				**1.00**	0.23	18	**1.02**		1
Polyzois and Charnvarnichborikarn (1993)	**0.87**	0.08	47	**1.03**	0.16	38	**0.95**	0.12	60	**1.09**	0.11	25	**0.92**	0.12	60	**1.05**	0.10	25
All data	**0.91**	0.14	143	**1.04**	0.15	44	**1.00**	0.15	162	**1.09**	0.11	25	**0.97**	0.14	156	**1.08**	0.12	31

Design method:	C1: Effective Width with L+E and D+E Check						C2: Hand-Direct Strength with L+E & D+E						C3: Numerical Direct Strength L+E & D+E					
Limit state[a]	L+E			D+E			L+E			D+E			L+E			D+E		
Test to predicted[b]	**mean**	std	*n*	**mean**	std	*n*	**mean**	std	*n*	**mean**	std	*n*	**mean**	std	*n*	**mean**	std	*n*
Loughlan (1979)	**0.97**	0.04	12	**0.94**		1	**1.12**	0.05	12	**0.94**		1	**1.09**	0.05	12	**1.00**		1
Miller and Peköz (1994)	**0.85**	0.04	8	**0.93**	0.03	5	**1.01**	0.07	13				**0.99**	0.06	12	**1.38**		1
Mulligan (1983)	**0.84**	0.12	32	**0.74**		1	**0.94**	0.12	33				**0.92**	0.13	33			
Mulligan stub col.	**1.04**	0.06	18	**1.10**	0.07	6	**1.15**	0.09	24				**1.10**	0.10	18	**1.26**	0.06	6
Thomasson (1978)	**1.04**	0.25	14	**0.97**	0.10	5	**1.01**	0.25	14	**1.04**	0.09	5	**1.07**	0.30	9	**1.00**	0.13	10
Polyzois and Charnvarnichborikarn (1993)	**0.87**	0.08	47	**1.07**	0.17	38	0.96	0.12	57	**1.12**	0.15	28	**0.92**	0.12	60	**1.12**	0.10	25
All data	**0.91**	0.14	131	**1.04**	0.16	56	**1.00**	0.15	153	**1.10**	0.15	34	**0.97**	0.15	144	**1.11**	0.14	43

Design method:	D1: Effective Width L+E, D+E, and L+D Check									D2: Hand-Direct Strength L+E, D+E, & L+D									D3: Num. Direct Strength L+E, D+E, & L+D								
Limit state[a]	L+E			D+E			L+D			L+E			D+E			L+D			L+E			D+E			L+D		
Test to predicted[b]	**mean**	std	*n*	**mean**	std	*n*	**mean**	std	*n*	**mean**	std	*n*	**mean**	std	*n*	**mean**	std	*n*	**mean**	std	*n*	**mean**	std	*n*	**mean**	std	*n*
Loughlan (1979)							**1.25**	0.15	13							**1.43**	0.21	13							**1.41**	0.20	13
Miller and Peköz (1994)							**1.46**	0.12	13							**1.77**	0.14	13							**1.86**	0.22	13
Mulligan (1983)	**0.94**	0.16	7				**0.94**	0.13	26	**1.01**	0.16	7				**1.07**	0.17	26	**0.99**	0.21	4				**1.09**	0.19	29
Mulligan sub col.							**1.47**	0.21	24							**1.64**	0.37	24							**1.76**	0.50	24
Thomasson (1978)	**1.04**	0.25	14				**1.12**	0.24	5	**1.03**	0.27	12	**1.08**	0.04	2	**1.21**	0.27	5	**1.07**	0.30	9	**0.95**	0.14	5	**1.27**	0.28	5
Polyzois and Charnvarnichborikarn (1993)	**0.86**	0.05	11				**1.14**	0.22	74	**0.88**	0.07	11				**1.25**	0.24	74							**1.24**	0.29	85
All data	**0.96**	0.20	32				**1.19**	0.26	155	**0.97**	0.20	30	**1.08**	0.04	2	**1.34**	0.33	155	**1.05**	0.27	13	**0.95**	0.14	5	**1.35**	0.39	169

[a]L=Local buckling, D=distortional buckling, E=Euler (overall) buckling, L+E=limit state that consider local buckling interaction with Euler (overall) buckling, etc.

[b]Test to predicted ratios are broken down by the controlling limit state.

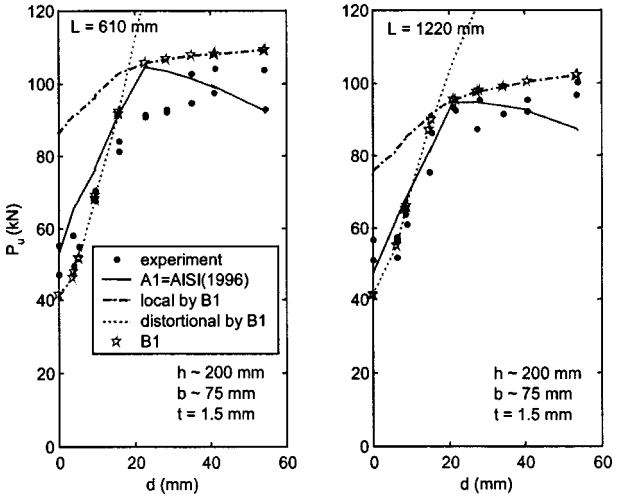

Fig. 5. Performance of method A1 and B1 for sample of zed columns

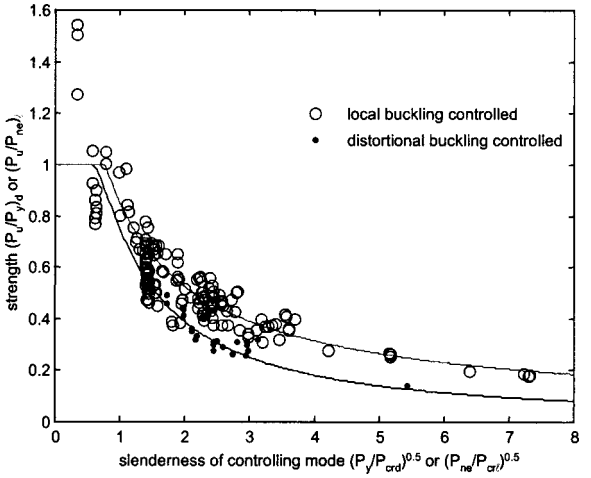

Fig. 6. Method B3: slenderness versus strength for lipped channel and zed columns

benefit from the inclusion of distortional buckling into current specification methods, even this simple additional check.

Alternative Effective Width Method (B1)

Current design specifications use an element based effective width method for determining strength. However, buckling predictions are not always based on simple element methods [i.e., Eqs. (1)–(3)], but rather on empirical corrections to these expressions that include certain aspects of local buckling interaction and distortional buckling. If distortional buckling is treated separately from local buckling then many of these empirical corrections can be removed and simple expressions [Eqs. (1)–(3)] may be used for local buckling. This basic approach is investigated in methods B1, C1, and D1—considering various levels of interaction among the modes.

Method B1 employs a separate check for distortional buckling and considers local and Euler buckling interaction. The predicted strength, (e.g.), in Fig. 5 for a series of lipped zed column tests, is the minimum of the distortional buckling curve and the local buckling curve. Strength in the distortional mode is well predicted, but strength in the local mode still suffers from systematic error due to ignoring web/flange interaction. Method B1 provides a reasonable upper bound solution and works as well as existing design methods (A1), peculiarities of the strength prediction as lip length is increased are removed, and explicit separation of local and distortional modes is more consistent with observed behavior.

Direct Strength Method (B2 and B3)

The direct strength methods are based on the use of separate strength (column) curves for local and distortional buckling. Method B2 relies on closed-form hand methods for predicting the local and distortional buckling stress [Eqs. (4)–(6) and (7)–(15)], while method B3 uses numerical methods (finite strip analysis) for the elastic buckling prediction. Otherwise the two methods are the same. For lipped channel and zed section data the performance of the strength curves is shown as slenderness vs. strength in Fig. 6 and summarized in Table 4. The method performs well, and given typical scatter in column data, appears to be a good predictor over a wide range of slenderness. The increased accuracy of the method (over methods A1, A2, and B1) occurs due to improvements in the local buckling prediction. Again using the zed column data as an example, the local buckling curves for direct strength methods B2 or B3 (Fig. 7) can be compared with the element based method B1 or A1 (Fig. 5) to demonstrate that local web/flange interaction is the key difference in the methods. Examination of the data with respect to h/t, $h/t \cdot h/b$, and distortional slenderness, as well as other variables reveals no systematic error. The direct strength method postulates that if elastic critical buckling loads in the local and distortional mode are known this information is enough to determine the member strength—for this data, the notion appears validated.

Overall Methods Considering Distortional and Euler Interaction (C1, C2, C3)

Design methods C1, C2, and C3 are nearly identical to their counterparts; methods B1, B2, and B3, respectively, except that in the strength calculation for distortional buckling interaction with Euler buckling is considered. For the lipped channel and zed sections little overall difference occurs when distortional and Euler

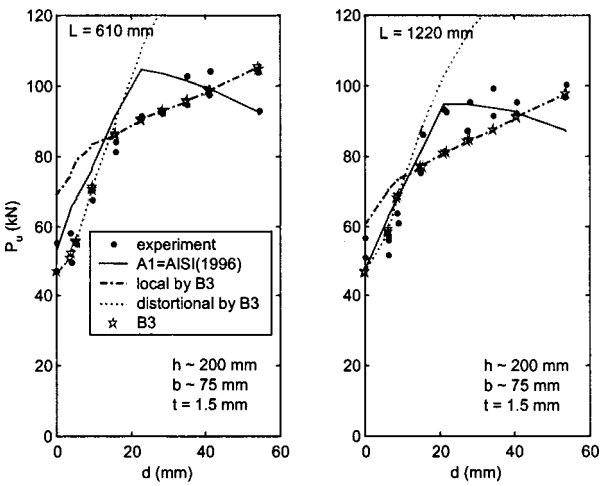

Fig. 7. Performance of method B3 for sample of zed columns

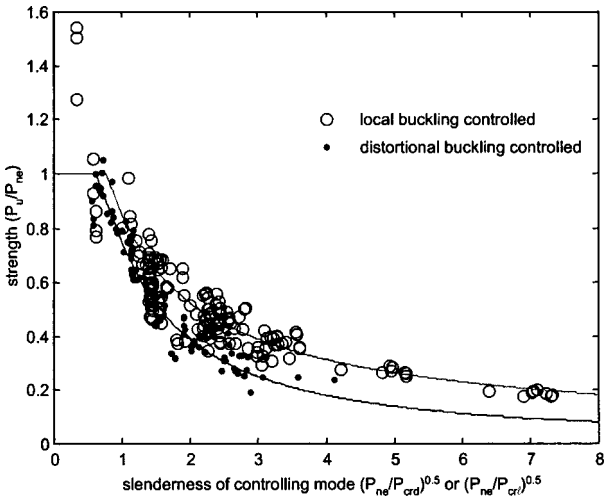

Fig. 8. Method C3: slenderness versus strength for all available column data (channels, zeds, channels with intermediate web stiffeners, racks, racks with compound lips)

interaction is considered. Local buckling predictions are unchanged and distortional buckling predictions are slightly more conservative. Interaction of distortional buckling with Euler buckling cannot be definitively recognized nor rejected on this basis.

For members with short lip length (small *d*) distortional and Euler interaction seems plausible: deformations and wavelengths of the distortional mode are similar to the local mode, which is known to interact with Euler buckling in pin-ended columns. However, for members with large *d*, or with intermediate stiffeners or other modifications that cause the wavelength in the distortional mode to be significantly longer than the local mode; interaction with Euler buckling seems less plausible. For example, the experimental data on channels with intermediate stiffeners and racks with large compound lips (Fig. 3) successfully ignores Euler interaction. Nonetheless, including Euler interaction in the distortional buckling calculation is conservative and does not further complicate the procedure, since it must already be considered for the local mode.

Direct Strength Considering Distortional and Euler Interaction (C3)

The performance of the direct strength method (C3) for the lipped channel and zed column data as well as the Thomasson (1978) data with web stiffeners and the Univ. of Sydney data is shown in Fig. 8. Test to predicted ratios for the channel and zed sections are given in Table 4. For Thomasson's data, with 1 and 2 web stiffeners and an attached bar restricting the symmetrical distortional mode, the average test to predicted ratio is 0.94 with a standard deviation of 0.13, for the University of Sydney data the test to predicted ratio is 1.01 with a standard deviation of 0.07. Though scatter certainly exists, the direct strength approach is viable as a general method for prediction of the strength of cold-formed steel columns in local, or distortional buckling with consideration of interaction with Euler buckling.

Methods Considering Local and Distortional Interaction (D1, D2, D3)

The ''D'' methods (D1, D2, and D3) allow local and distortional interaction by setting the limiting stress for local buckling calculations to the inelastic distortional buckling stress. The methods perform poorly. In the majority of cases local plus distortional interaction is identified as the controlling limit state, but predicted strengths are overly conservative. Interaction may still exist between these two modes, but in the available data, local and distortional interaction does not appear significant. Based on this finding it is recommended that local and distortional interaction be ignored for routine design. One cautionary note, other members may indicate interaction between these two modes, e.g., limited evidence exists showing that for perforated rack columns that local and distortional modes may interact (Baldassino and Hancock 1999).

Discussion

Reliability

The reliability of the examined design methods is assessed by calculating the resistance factor (ϕ) for a reliability (β) of 2.5 via the guidelines of Sec. *F* in AISI (1996). Variability is relatively high, and the resulting ϕ factors are approximately consistent with current practice of $\phi = 0.85$. AISI (1996), method A1, has a ϕ of 0.82, the effective width methods B1 and C1 have $\phi = 0.81$, the closed-form (hand) direct strength methods B2 and C2 have $\phi = 0.86$, and the numerical direct strength methods B3 and C3 have $\phi = 0.84$. If local and distortional buckling are treated as different limit states then two different ϕ factors may be considered. Experimental data suggests lower ϕ factors for local buckling than distortional buckling; however, this does not reflect variability in the data (Table 4 shows the variability in the two methods is generally about the same—if not a little higher for distortional failure modes) but rather differences in the mean test to predicted ratios for the two modes. Although numerical studies suggest distortional failures have a greater imperfection sensitivity and thus lower ϕ factors are needed, available experimental data does not currently justify such a change. Continued use of $\phi \sim 0.85$ appears appropriate for cold-formed steel columns.

Restriction of Distortional Mode

In considering local, distortional, and Euler buckling a factor not explicitly discussed is the restriction of the distortional mode through bracing or other means. In common applications local buckling cannot be significantly restricted because it occurs at short wavelengths. Consideration of braced length is primarily a determination of Euler buckling. However, little work has been completed on the effect of restriction of the distortional mode. In many cases, attachments to other members (e.g., sheathing), as well as discrete braces may hinder the distortional mode and thus increase the strength.

Restriction of distortional buckling in Thomasson's tests (with bars connecting the flanges) was modeled by using the higher f_{crd} from antisymmetric distortional buckling [Fig. 4(c)] instead of symmetric distortional buckling [Fig. 4(b)]. General guidance on including bracing or other attachments that restrict the distortional mode is lacking. For discrete braces the best current practice is to compare the unbraced length (L_m) with the half-wavelength of the mode [L_{cr} of Eq. (15)]. If $L_m < L_{\text{cr}}$ it may be used in place of L_{cr} in Eqs. (11)–(14). Alternatively numerical analysis considering the bracing itself, or performed at the unbraced length directly, may be completed. The bracing should restrict rotation of

the flange and cause the distortional buckling wave to occur within the unbraced segment.

Recommendations for Column Design

Two methods are recommended for thin-walled column design: C1 and C2/C3. If current design practice continues with element based effective width procedures then method C1 provides the best alternative to current practice. C1 removes complicated empirical expressions for local buckling and replaces them with simple formulas [Eqs. (1)–(3)] and adds an explicit check on distortional buckling. Compared with current practice (method A1, AISI 1996) adoption of C1 favors members with longer lips (higher d/b), and discourages members with small lips, as members with $d/b<0.2$ may see significant strength reductions. For common lipped channel and zed members the average change in predicted strength is less than 1%. A unified approach may still be maintained as similar procedures have been shown to work for flexural members as well (Schafer and Peköz 1999).

Whether implemented as a traditional hand method (C2) or one that allows rational analysis for elastic buckling determination (C3) the direct strength method provides a reliable alternative design procedure for thin-walled compression members. Adoption of the direct strength method holds several advantages over current methods: calculations do not have to be performed for individual elements, interaction of the elements in local buckling is accounted for, distortional buckling is explicitly treated as a unique limit state, a means for introducing rational analysis through numerical prediction of elastic buckling is provided, and a general method for design is provided for members with stiffener configurations or other geometries in which current rules are inapplicable.

The direct strength methods (e.g., C3) can provide markedly different strength predictions than current practice [method A1—AISI (1996)]: in the studied members of lipped channels and zeds the predicted strength for individual members may be as much as 16% higher, but on average entails a strength loss of 7%. Compared to current practice, narrow members (high h/b) with slender webs (high h/t) and short lips (low d/b) will be specifically discouraged. Members with longer lips (higher d/b) are encouraged. The direct strength method integrates known behavior into a design procedure, removes systematic error, and has a mean test to predicted ratio of 1.01.

Conclusions

Behavior and design of thin-walled, cold-formed steel columns requires consideration of local, distortional, and Euler (i.e., flexural or flexural-torsional) buckling. Accurate closed-form methods are provided for prediction of local buckling, including interaction, and distortional buckling. Current design methods ignore local buckling interaction and do not explicitly consider distortional buckling. Ignoring local buckling interaction leads to systematic error in strength prediction. Experimental and numerical studies indicate that postbuckling strength in the distortional mode is less than in the local mode.

In pin-ended lipped channel and zed columns, local and Euler interaction is well established. Comparisons with experimental data indicate local and distortional interaction is not significant, but are inconclusive regarding distortional and Euler interaction—for now it is proposed to include this interaction in design. A direct strength method (C2 and/or C3) is proposed for column design. The method uses separate column curves for local buckling [Eq. (19)] and distortional buckling [Eq. (16)], with the slenderness and maximum capacity in each mode controlled by consideration of Euler buckling [Eq. (18)]. The method considers all the buckling modes in a consistent manner, does not require effective width calculations, and demonstrates that numerical elastic buckling solutions (e.g., finite strip) may be used as the key input to determining the strength of a large variety of thin-walled compression members.

Acknowledgments

The sponsorship of the American Iron and Steel Institute (AISI) in funding this research is gratefully acknowledged. Comments from members of the AISI Committee on Specifications including Roger Brockenbrough, Helen Chen, Jim Crews, Don Johnson, Teoman Peköz, Tom Trestain, and others on the committee are also gratefully acknowledged.

References

AISI. (1996). *Cold-Formed Steel Design Manual*, American Iron and Steel Institute, Washington, D.C.

Baldassino, N., and Hancock, G. (1999). ''Distortional buckling of cold-formed steel storage rack section including perforations.'' *Proc., 4th Int. Conf. on Steel and Aluminum Structures* (ICSAS '99), Espoo, Finland.

Cheung, Y. K., and Tam, L. G. (1998). *Finite Strip Method*, Chemical Rubber, Boca Raton, Fla.

Desmond, T. P., Peköz, T., and Winter, G. (1981). ''Edge stiffeners for thin-walled members.'' *J. Struct. Div., ASCE,* 107(ST2), 329–353.

Hancock, G. J., Kwon, Y. B., and Bernard, E. S. (1994). ''Strength design curves for thin-walled sections undergoing distortional buckling.'' *J. Constr. Steel Res.,* 31(2-3), 169–186.

Hancock, G. J., Rogers, C. A., and Schuster, R. M. (1996). ''Comparison of the distortional buckling method for flexural members with tests.'' *Proc., 13th Int. Specialty Conf. on Cold-Formed Steel Structures*, St. Louis.

Kwon, Y. B., and Hancock, G. J. (1992). ''Tests of cold-formed channel with local and distortional buckling.'' *J. Struct. Eng.,* 118(7), 1786–1803.

Lau, S. C. W., and Hancock, G. J. (1987). ''Distortional buckling formulas for channel columns.'' *J. Struct. Eng.,* 113(5), 1063–1078.

Loughlan, J. (1979). ''Mode interaction in lipped channel columns under concentric or eccentric loading.'' PhD thesis, Univ. of Strathclyde, Glasgow.

Miller, T. H., and Peköz, T. (1994). ''Load-eccentricity effects on cold-formed-steel lipped-channel columns.'' *J. Struct. Eng.,* 120(3), 805–823.

Mulligan, G. P. (1983). ''The influence of local buckling on the structural behavior of singly-symmetric cold-formed steel columns.'' PhD thesis, Cornell Univ., Ithaca, N.Y.

Peköz, T. (1987). ''Development of a unified approach to the design of cold-formed steel members.'' *Research Rep. No. CF 87-1*, American Iron and Steel Institute, Washington, D.C.

Polyzois, D., and Charnvarnichborikarn, P. (1993). ''Web-flange interaction in cold-formed steel Z-section columns.'' *J. Struct. Eng.,* 119(9), 2607–2628.

Schafer, B. W. (1997). ''Cold-formed steel behavior and design: Analytical and numerical modeling of elements and members with longitudinal stiffeners.'' PhD dissertation, Cornell Univ., Ithaca, N.Y.

Schafer, B. W. (2000). ''Distortional buckling of cold-formed steel columns: Final report.'' Sponsored by the American Iron and Steel Institute, Washington, D.C.

Schafer, B. W., and Peköz, T. (1998a). ''Computational modeling of cold-formed steel: Characterizing geometric imperfections and residual

stresses.'' *J. Constr. Steel Res.*, 47(3).
Schafer, B. W., and Peköz, T. (1998b). ''Direct strength prediction of cold-formed steel members using numerical elastic buckling solutions.'' *14th Int. Specialty Conf. on Cold-Formed Steel Structures*, St. Louis.
Schafer, B. W., and Peköz, T. (1999). ''Laterally braced cold-formed steel flexural members with edge stiffened flanges.'' *J. Struct. Eng.*, 125(2), 118–127.
Thomasson, P. (1978). ''Thin-walled C-shaped panels in axial compression.'' Swedish Council for Building Research, D1 1978, Stockholm, Sweden.
Yu, W. W. (2000). *Cold-Formed Steel Design*, Wiley, New York.